

Ultrastrong coupling limit to quantum mean force Gibbs state for anharmonic environment

Prem Kumar^{1,2} and Sibasish Ghosh^{1,2}

¹⁾*Optics and Quantum Information Group, The Institute of Mathematical Sciences, C.I.T. Campus, Taramani, Chennai 600113, India.*

²⁾*Homi Bhabha National Institute, Training School Complex, Anushakti Nagar, Mumbai 400094, India*

(*Electronic mail: premkr@imsc.res.in)

(Dated: 20 November 2024)

The equilibrium state of a quantum system can deviate from the Gibbs state if the system-environment (SE) coupling is not weak. An analytical expression for this mean force Gibbs state (MFGS) is known in the ultrastrong coupling (USC) regime for the Caldeira-Leggett (CL) model that assumes a harmonic environment. Here, we derive analytical expressions for the MFGS in the USC regime for more general SE models. For all the generalized models considered here, we find the USC state to be diagonal in the basis set by the SE interaction, just like in the CL case. While for the generic model considered, the corresponding USC-MFGS is found to alter from the CL-result, we do identify a class of models more general than the CL model for which the CL-USC result remains unchanged. We also provide numerical verification for our results. These results provide key tools for the study of strong coupling quantum thermodynamics and several quantum chemistry and biology problems under more realistic SE models, going beyond the CL model.

I. INTRODUCTION

Non-negligible system-environment (SE) coupling can cause the equilibrium state of a system to deviate from the textbook Gibbs state.^{1,2} The concept of Mean Force Gibbs State (MFGS) has been developed to capture the idea of this generalized equilibrium state, and has historically seen a lot of application in the field of chemistry^{3–6} and, more recently, to the theory of strong coupling quantum thermodynamics.^{1,7–13} Many of these approaches to calculate the quantum MFGS assume the Caldeira-Leggett (CL) model for the system and the environment, in which the environment is modelled as a set of harmonic oscillators coupled to the system.

The harmonic environment approximation has been widely successful in capturing the behavior of a variety of physical systems.^{14–31} Yet, advancement in experimental techniques and more detailed theoretical considerations have shown the inadequacy of the harmonic environment approximation, sparking numerous studies on open quantum system with anharmonic environment.^{32–44} For example, for electron transfer happening in the presence of strongly coupled low-frequency intramolecular modes or an environment consisting of nonpolar liquids, the harmonic approximation is known to fail.^{32–35,39–42} It is hence worth investigating the MFGS result for SE models beyond the CL model.

If \hat{H}_{SE} denotes the full Hamiltonian of a system and environment, then the MFGS is formally defined as^{45,46}

$$\hat{\rho} = Z^{-1} \text{Tr}_E \left[e^{-\beta \hat{H}_{SE}} \right], \quad (1)$$

where Z is an appropriate normalization constant.

For the CL model, analytical expression for the MFGS in ultrastrong coupling (USC) regime has been determined for continuous variable (CV) systems^{47,48} and, more recently, for a more general CL model (consisting of an arbitrary system Hamiltonian and coupling-operator).⁴⁵ Moreover, this state is also confirmed to be the steady state of an ultrastrong coupling master equation.⁴⁹

The USC-MFGS acts as a good indicator for the deviation of the MFGS from the textbook Gibbs state at large coupling. However, since this result is only valid for the CL model, its applicability is significantly limited. It also remains uncertain as to which aspects of the USC result are artifacts of the specific structures of the CL model, and which aspects might persist when the model is generalized. Here, we attempt to address this issue by studying the USC-MFGS for models beyond the CL model.

We find that for all the SE models considered by us, one of the core features of the CL-USC result, that the MFGS is diagonal in the basis set by the SE interaction, remains intact, although the functional form of the MFGS does get affected. For example, the most general extension of the CL model considered by us, which we call the GCL model, shows such deviations from the CL-USC result. Within the GCL model, we identify a subclass of models, which we call the GCL2 model, for which the CL-USC result remains exactly valid. Finally, we derive an analytical expression for the USC-MFGS for another class of model (distinct from the GCL model), the so-called Zwanzig model^{50–53}, and find that the corresponding USC state, although still diagonal in the basis set by the SE interaction, has qualitative distinctions from the GCL2-USC result.

In Section II, we rederive the known USC-MFGS result for the CL model⁴⁵ using the path integral approach, to illustrate the method that we will be using to generalize the same result. Section III contains the derivation of the USC result for the GCL model, while Section III A acts as a special case of the same derivation for the more restricted GCL2 model. Finally, in Section IV, we provide the USC-MFGS derivation for the Zwanzig model. Section V provides some numerical verifications of the analytical results derived here, and Section VI provides conclusions and future directions.

II. USC-MFGS IN CL MODEL

Consider a typical CL model in which a generic quantum system, with free Hamiltonian \hat{H}_S , has a one-to-one interaction with a set of harmonic oscillators that are uncoupled from each other. The full SE Hamiltonian is hence given by

$$\hat{H}_{SE} = \hat{H}_S + \hat{H}_I, \quad (2)$$

$$\hat{H}_I = \sum_k \left[\frac{\hat{p}_k^2}{2m_k} + \frac{1}{2} m_k \omega_k^2 (\hat{q}_k - \alpha_k \hat{A})^2 \right], \quad (3)$$

where \hat{A} is a generic system operator through which the system couples to the environment (which from now onwards we will refer to as ‘system coupling-operator’) and

$$\alpha_k \equiv \frac{c_k}{m_k \omega_k^2}, \quad (4)$$

where m_k and ω_k are the mass and frequency of the k th harmonic oscillator and c_k is the corresponding SE coupling strength. For a CV system, typically we have $\hat{A} = \hat{q}$, where \hat{q} is the position operator of the system; while for the spin-Boson model, \hat{A} is taken to be a Pauli matrix.^{28–30}

The MFGS (Eq. 1) can be calculated using the Feynman path integral⁵⁴ in the basis of the operator \hat{A} by evolving the system and the environment in the ‘imaginary time’ by an amount β and then tracing over the environment degrees of freedom.^{14,28}

Note a subtlety that arises when the system coupling-operator \hat{A} has degeneracy, and hence each of its eigenstates is not uniquely labelled by an eigenvalue. To fix this problem, let us introduce an operator $\hat{\phi}$ that lifts the degeneracy in \hat{A} . That is, $[\hat{\phi}, \hat{A}] = 0$ and $\hat{A} + \hat{\phi}$ has no degeneracy. The final result will not depend upon the particular choice of $\hat{\phi}$. Without any loss of generality and for convenience, we will also assume that $\hat{\phi}$ is itself non-degenerate, so that its eigenvalues, (a, b) , can be used as a unique label to express the system’s reduced density matrix elements as $\hat{\rho}(a, b)$.

Let a generic imaginary time path be denoted as $\{A(t), \phi(t), q_k(t)\}$, where $A(t) \in \{A_i\}$, $\phi(t) \in \{\phi_i\}$, and $q_k(t) \in \{q_{ki}\}$, where $\{A_i\}$, $\{\phi_i\}$ and $\{q_{ki}\}$ are the sets of eigenvalues of operators \hat{A} , $\hat{\phi}$ and \hat{q}_k , respectively. We emphasize here that $A(t)$ denotes a path that the system can take in the path integral and should not be confused to mean that the system coupling-operator, \hat{A} , has a time dependence. In fact, \hat{A} has been assumed to be time-independent throughout this paper.

Now, let $S_S[A(t), \phi(t)]$ and $S_I[A(t), q_k(t)]$ represent the imaginary time action corresponding to \hat{H}_S and \hat{H}_I , respectively. Note how S_I is not a function of $\phi(t)$ while S_S is. This is because while \hat{H}_S is an arbitrary system operator, \hat{H}_I has system dependence only through the operator \hat{A} , and hence the corresponding action, S_I , cannot distinguish within the degenerate subspace of \hat{A} , which removes the $\phi(t)$ dependence.

Also note that the paths $A(t)$ and $\phi(t)$ are not independent of each other. That is, $A(t)$ and $\phi(t)$ denote some eigenvalues of the operators \hat{A} and $\hat{\phi}$, respectively, such that one can find a common eigenvector $|v(t)\rangle \equiv |A(t), \phi(t)\rangle$ such that

$\hat{A}|v(t)\rangle = A(t)|v(t)\rangle$ and $\hat{\phi}|v(t)\rangle = \phi(t)|v(t)\rangle$. But we can always treat $A(t)$ and $\phi(t)$ as independent of each other if we assume that the action $S_S[A(t), \phi(t)]$ is constructed in such a manner that, given some $A(t)$, it rules out all unphysical possibilities for the path $\phi(t)$ by assigning the corresponding action an infinite weight. For all the arguments in this paper, we *don’t* need to go into any further details on how to construct such a functional $S_S[A(t), \phi(t)]$.

The full SE path integral is given as

$$\hat{\rho}(a, b, a_k, b_k) = \tilde{Z}^{-1} \left(\prod_k \int_{a_k}^{b_k} \mathcal{D}q_k(t) \right) \int_{\bar{a}}^{\bar{b}} \mathcal{D}A(t) \times \int_a^b \mathcal{D}\phi(t) e^{-S_S[A(t), \phi(t)] - S_I[A(t), q_k(t)]}. \quad (5)$$

Here \tilde{Z} is the overall normalization factor and a, b, a_k, b_k, \bar{a} , and \bar{b} correspond to $\phi(0), \phi(\beta), q_k(0), q_k(\beta), A(0)$, and $A(\beta)$, respectively. Tracing over the environment will now give us the MFGS as

$$\hat{\rho}_{\text{USC}}(a, b) = \left(\prod_k \int_{-\infty}^{\infty} da_k \right) \hat{\rho}(a, b, a_k, a_k) \quad (6)$$

$$= \tilde{Z}^{-1} \int_{\bar{a}}^{\bar{b}} \mathcal{D}A(t) \int_a^b \mathcal{D}\phi(t) e^{-S_S[A(t), \phi(t)]} I[A(t)]. \quad (7)$$

Here $I[A(t)] \equiv \prod_k I_k[A(t)]$ is called the influence functional^{14,28}, where $I_k[A(t)]$ encapsulates the effect of the k th environment particle only and is defined as

$$I_k[A(t)] = \int_{-\infty}^{\infty} dx \int_x^x \mathcal{D}q_k(t) e^{-S_k[q_k(t), A(t)]}. \quad (8)$$

Here the action, S_k , is defined as

$$S_k[q_k(t), A(t)] \equiv \int_0^\beta dt \left\{ \frac{m_k}{2} \dot{q}_k(t)^2 + \frac{m_k \omega_k^2}{2} (q_k(t) - \alpha_k A(t))^2 \right\}. \quad (9)$$

The explicit expression for $I[A(t)]$ for CL model^{14,28} can be used to derive the CL-USC result.^{47,55} But here, since we need to eventually generalize this result beyond the CL model, we will derive the expression for the USC-MFGS without explicitly evaluating $I[A(t)]$ for any specific model.

Let us choose an arbitrarily large but finite length scale Δ such that whenever $|q_k(t) - \alpha_k A(t)| > \Delta$ for any t , the potential energy (PE) cost of the corresponding path, $q_k(t)$, will be very high, and hence its contribution to the path integral will be negligible. We can hence write, for all paths $q_k^*(t)$ that *do* have significant contribution to the path integral,

$$|q_k^*(t) - \alpha_k A(t)| < \Delta. \quad (10)$$

Let us define

$$\langle A \rangle \equiv \frac{1}{\beta} \int_0^\beta dt A(t), \quad (11)$$

$$\langle A^2 \rangle \equiv \frac{1}{\beta} \int_0^\beta dt A(t)^2, \quad (12)$$

$$\sigma_A^2 \equiv \langle A^2 \rangle - \langle A \rangle^2. \quad (13)$$

Then, in Appendix. A, we have proven that if $\sigma_A^2 \gg \Delta^2/\alpha_k^2$, then

$$\frac{1}{\beta} \int_0^\beta dt \dot{q}_k^*(t)^2 \geq \alpha_k^2 \mu \frac{\sigma_A^2}{\beta^2}. \quad (14)$$

Here $\mu > 0$ is some constant. Now, note that in the USC limit, defined as

$$\lim c_k \rightarrow \infty, \quad (15)$$

we have $\alpha_k \rightarrow \infty$ (Eq. 4). Hence, in this limit, unless $\sigma_A = O(\Delta/\alpha_k)$, the RHS in Eq. 14 diverges, causing the kinetic term $\dot{q}_k^*(t)^2$ in the action $S_k[q_k(t), A(t)]$ (Eq. 9) to diverge. Hence, in the USC limit (Eq. 15), paths $q_k^*(t)$ (which have been defined to have convergent PE cost) will have divergent kinetic energy cost unless σ_A vanishes, or in other words, unless we have

$$A(t) = A(0) = \tilde{a}, \quad \text{for some constant } \tilde{a}. \quad (16)$$

As we will see, Eq. 16 will greatly simplify the evaluation of the MFGS path integral (Eq. 7). But before getting into that, we need to address a subtlety. If the system lives in a discrete Hilbert space, then $A(t)$ may not be continuous and differentiable everywhere, leading to potential mathematical irregularities. Although the results and proofs in this paper only require the paths $A(t)$ to be square integrable (and not continuous and differentiable), we note that these mathematical irregularities can be addressed by substituting $A(t)$ with a continuous and differentiable function $X(t)$ that closely approximates it, such that the induced error, $|I[A(t)] - I[X(t)]|$, is arbitrarily small. For instance, Fig. 1 illustrates how $X(t)$, using a cubic polynomial near $t = 1$, smoothly approximates $A(t)$'s discrete jump.

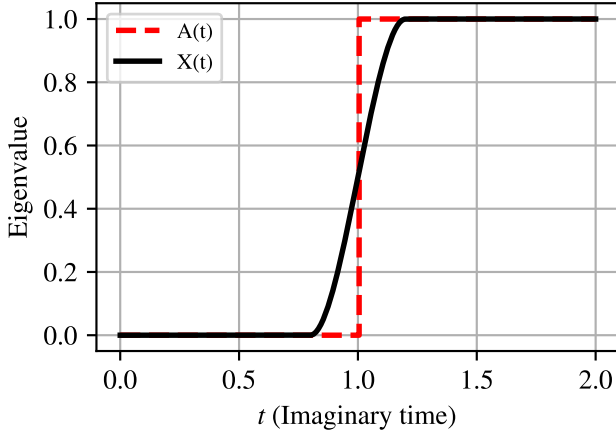


FIG. 1. Approximating a piecewise constant function, $A(t)$, with a continuous and differentiable function $X(t)$. The function $X(t)$ is equal to $A(t)$ everywhere except near the discontinuous jump in $A(t)$ (when $1 - \delta < t < 1 + \delta$, for $\delta = 0.2$). Near $t = 1$, $X(t)$ takes the form of a cubic function, $f(t') = a_0 + a_1 t' + a_3 t'^3$, with $t' = t - 1$, $a_0 = 1/2$, $a_1 = 3/(4\delta)$ and $a_3 = -1/(4\delta^3)$. This means that we have $\lim_{\delta \rightarrow 0} X(t) = A(t)$.

Now, given Eq. 16, the expression for the influence functional (Eq. 8) simplifies as

$$I_k[\tilde{a}] = \int_{-\infty}^{\infty} dx \int_x^x \mathcal{D}q_k(t) e^{-S_k[q_k(t), \tilde{a}]} \quad (17)$$

$$= \int_{-\infty}^{\infty} dx \int_{x-\alpha_k \tilde{a}}^{x-\alpha_k \tilde{a}} \mathcal{D}x_k(t) e^{-S_k[x_k(t), 0]} \quad (18)$$

$$= \int_{-\infty}^{\infty} dx \int_x^x \mathcal{D}x_k(t) e^{-S_k[x_k(t), 0]} \quad (19)$$

$$= I_k, \quad \text{which is independent of } \tilde{a}. \quad (20)$$

Here in Eq. 18, we defined $x_k(t) \equiv q_k(t) - \alpha_k \tilde{a}$ and we have used the relation $S_k[q_k(t), \tilde{a}] = S_k[x_k(t), 0]$ (Eq. 9). We hence have that $I[\tilde{a}] \equiv I$ is independent of \tilde{a} . Hence, the only contribution of the environment side path integral is to eliminate all the system side paths that do not satisfy Eq. 16. This means that jumps within a degenerate subspace are still allowed and with equal weight as far as the environment side path integral is concerned. Therefore, the full MFGS path integral (Eq. 7) simplifies as

$$\hat{\rho}_{\text{USC}}(a, b) = \tilde{Z}^{-1} I \int_a^b \mathcal{D}\phi(t) \exp\{-S_S[\tilde{a}, \phi(t)]\}. \quad (21)$$

Here a and b are the eigenvalues of the operator $\hat{\phi}$ and \tilde{a} is the eigenvalue of \hat{A} .⁵⁶ Then, the USC-MFGS is given as

$$\hat{\rho}_{\text{USC}} = Z^{-1} \exp\{-\beta \tilde{H}\}, \quad (22)$$

$$\tilde{H} \equiv \sum_i \hat{P}_i \hat{H}_S \hat{P}_i. \quad (23)$$

Here \hat{P}_i is the projection operator on the i th eigensubspace of the system coupling-operator, \hat{A} , and Z is the normalization constant. Eq. 22 is equivalent to the USC-MFGS derived by Cresser and Anders⁴⁵ using perturbation theory, and reduces to the USC-MFGS derived earlier for a CV system.⁴⁷ Note that the derivation provided in this section is applicable for a generic CL model, discrete or continuous. See Appendix. D for more details.

III. USC-MFGS FOR GENERALIZED CALDEIRA-LEGGETT MODEL

The generalization of the CL model has been considered by several authors^{34,36-38,41,42} and can be characterized by an interaction Hamiltonian, \hat{H}_I (Eq. 3), of the form

$$\hat{H}_I = \sum_k \left[\frac{\hat{p}_k^2}{2m_k} + V_k(\hat{q}_k, c_k \hat{A}) \right]. \quad (24)$$

Here $V_k(x, y)$ is a potential function bounded from below with a constraint that it should not renormalize the free effective system Hamiltonian \hat{H}_S .^{28,34,42,57} This is usually ensured by adding a so-called counter term in the potential, $V_k(x, y)$, which compensates for the shift in \hat{H}_S because of the environment. Here, we assume that such a counter term has already

been incorporated into $V_k(x, y)$, which translates into demanding that for a fixed value of y , if $x = \tilde{x}_k(y)$ is the point at which $V_k(x, y)$ has a global minimum, then^{28,42}

$$V_k(\tilde{x}_k(y), y) = 0. \quad (25)$$

These generalized CL models have been studied in various contexts. For instance, they have been used to explore the influence of an anharmonic environment on the non-Markovian dynamics of open systems⁴², to investigate certain condensed phase processes such as electron-transfer reactions^{36–38,41}, and to examine the electronic absorption spectra of chromophores embedded in condensed phase environments.³⁴

Here, we will generalize the derivation for the USC-MFGS provided in Section II to such a larger class of model that we call the Generalized Caldeira-Leggett (GCL) model. In order to proceed with the derivation of the USC-MFGS for such systems, we make two more physically motivated assumptions on the form of the potential $V_k(x, y)$ for our GCL model, i.e.,

$$\lim_{x \rightarrow \pm\infty} V_k(\tilde{x}_k(y) + x, y) = \Omega(|x|) \quad \forall y, \quad (26)$$

$$\frac{d}{dy} \tilde{x}_k(y) = \Omega(1). \quad (27)$$

Here, we have used the big Omega notation⁵⁸ which, given two non-negative functions $f(x)$ and $g(x)$ such that

$$g(x) = \Omega(f(x)), \quad (28)$$

is defined to imply that there exists a positive number C such that

$$g(x) \geq C f(x). \quad (29)$$

Also, here, $\tilde{x}_k(y)$ is assumed to be continuous and differentiable everywhere. We remark that the continuity of the function $\tilde{x}(y)$ is not affected by whether the system in question lives in a discrete dimensional Hilbert space or not because here we are treating $V_k(x, y)$ and $\tilde{x}(y)$ as generic functions that can act on continuous variables as well as discrete operators.

Justification for Eq. 26 is that keeping the system variable, y , fixed, if we move the environment variable x far away from its global minima point $\tilde{x}_k(y)$, then the value of the potential rises at least linearly with $|x - \tilde{x}_k(y)|$. That is, we assume that the system and environment variables are attractively coupled to each other.

Note that we can relax the assumption Eq. 27 to $d\tilde{x}_k(y)/dy \geq \lambda$ for an arbitrarily small but finite $\lambda > 0$, but we stick to the present form for simplicity. We can motivate this assumption as following: if we instead assume that $|d\tilde{x}_k(y)/dy| \approx 0$, then this would mean that for a large variation in y , $\tilde{x}_k(y)$ would be almost constant (i.e., $\tilde{x}_k(y) \approx x_0$) and for the corresponding value of the potential, we will have $V_k(x_0, y) \approx 0$ (Eq. 25). Hence, the assumption Eq. 27 is applicable whenever the interaction potential is sensitive to a large change in the variable y while x is held constant.

The expression for the action, $S_k[q_k(t), A(t)]$ (Eq. 8) for the GCL model now becomes,

$$S_k[q_k(t), A(t)] = \int_0^\beta dt \left\{ \frac{m_k}{2} \dot{q}_k(t)^2 + V_k(q_k(t), c_k A(t)) \right\}. \quad (30)$$

Eq. 26 implies that, for a fixed value of y , there is a (perhaps) large but essentially finite basin with length scale Δ about the position $x = \tilde{x}_k(y)$, such that all paths $q_k(t)$ that explore the region $|x - \tilde{x}_k(y)| > \Delta$ will have a PE cost so high that the contribution of these paths to the path integral will be negligible. Hence, for all paths $q_k^*(t)$ that *do* have a significant contribution to the path integral, we again have that

$$|q_k^*(t) - \tilde{x}_k(c_k A(t))| < \Delta. \quad (31)$$

Since $\tilde{x}(c_k A(t))$ is ultimately a function of t , we can define $\langle \tilde{x}_A \rangle$, $\langle \tilde{x}_A^2 \rangle$ and $\sigma_{\tilde{x}_A}^2$ analogous to Eqs. 11-13. Next, given Eq. 27, we prove in Appendix. B that

$$\sigma_{\tilde{x}_A}^2 \gtrsim c_k^2 \sigma_A^2. \quad (32)$$

Next, we note that if $\sigma_{\tilde{x}_A} \approx \Delta$, then $\sigma_A = O(\Delta/c_k)$, which vanishes in the USC limit (Eq. 15). Alternatively, if we instead assume that

$$\sigma_{\tilde{x}_A}^2 \gg \Delta^2, \quad (33)$$

then, using Eq. 31, in Appendix. A we prove that

$$\frac{1}{\beta} \int_0^\beta dt \dot{q}_k^*(t)^2 \geq \mu \frac{\sigma_{\tilde{x}_A}^2}{\beta^2} \quad (34)$$

$$\gtrsim c_k^2 \mu \frac{\sigma_A^2}{\beta^2}, \quad \text{using Eq. 32.} \quad (35)$$

Here $\mu > 0$. We have already encountered an inequality similar to Eq. 35 in the context of the CL model (Eq. 14). Again, we are led to a similar conclusion that in the USC limit (Eq. 15), paths $q_k^*(t)$ (which have been defined to have convergent PE cost) will have divergent kinetic energy cost unless σ_A vanishes. Therefore, again we have that $A(t) = A(0) = \tilde{a}$, for some constant \tilde{a} (Eq. 16). The expression for the influence functional (Eq. 8) hence simplifies as

$$I_k[\tilde{a}] = \int_{-\infty}^{\infty} dx \int_x^x \mathcal{D}q_k(t) e^{-S_k[q_k(t), \tilde{a}]} \quad (36)$$

$$\implies I[\tilde{a}] = \text{Tr} \left[e^{-\beta \hat{H}_I(\tilde{a})} \right]. \quad (37)$$

Here, for a scalar z , we have defined

$$\hat{H}_I(z) \equiv \sum_k [\hat{p}_k^2 / (2m_k) + V_k(\hat{q}_k, c_k z)]. \quad (38)$$

The expression for the full MFGS path integral (Eq. 7) then becomes

$$\hat{\rho}_{\text{USC}}(a, b) = \tilde{Z}^{-1} I[\tilde{a}] \int_a^b \mathcal{D}\phi(t) \exp \{-S_S[\tilde{a}, \phi(t)]\}. \quad (39)$$

Here a and b are eigenvalues of the operator $\hat{\phi}$ and \tilde{a} is eigenvalue of \hat{A} .⁵⁶ The USC-MFGS for GCL model is then given as

$$\hat{\rho}_{\text{USC}} = Z^{-1} \exp \{-\beta \tilde{H}\} \quad (40)$$

$$\tilde{H} \equiv \sum_i \hat{P}_i (\hat{H}_S + \hat{V}_0) \hat{P}_i. \quad (41)$$

Here Z is the normalization constant and \hat{P}_i is the projection operator on the i th degenerate subspace of the operator \hat{A} with eigenvalue A_i . Here, \hat{V}_0 is defined as

$$\hat{V}_0 = \sum_i \log \left(\text{Tr} \left(e^{-\beta \hat{H}_I(A_i)} \right) \right) \hat{P}_i, \quad (42)$$

where $\hat{H}_I(A_i)$ is as defined in Eq. 38.

The key takeaway here is that although the USC-MFGS for the GCL model is still diagonal in the basis of the system coupling-operator \hat{A} , the actual expression does deviate from the CL-USC result. Determining the actual expression for the GCL-USC result would involve calculating the Gibbs partition function corresponding to the free environment Hamiltonian, $\hat{H}_I(A_i)$, as a function of different values of A_i , and hence a closed form expression is not possible without further information on the form of $\hat{H}_I(A_i)$.

A. Special Case

Since the CL-USC result gets modified for the GCL case, we will now identify a subclass within the GCL model, which we will call the GCL2 model, for which the USC-MFGS result remains the same as that for the CL case, and hence can also be determined in closed form. To this end, let us assume a special form of the GCL model potential $V_k(x, y)$ (Eq. 24) as

$$V_k(x, y) = U_k(x - y). \quad (43)$$

Generalization of the CL model of this form has been considered before in literature³⁶ and physically reflects a symmetry in the potential such that we have $V_k(x + w, y + w) = V_k(x, y)$. The function $\tilde{x}_k(y)$, defined earlier, can now be expressed as

$$\tilde{x}_k(y) = y + x_k, \quad (44)$$

where x_k is some constant. Note how $d\tilde{x}_k(y)/dy = 1$ and hence the corresponding GCL model assumption (Eq. 27) is automatically satisfied here. The requirement that $U_k(x)$ does not renormalize the free system Hamiltonian (Eq. 25), on the other hand, translates into

$$U_k(x_k) = 0. \quad (45)$$

Similarly, the final GCL model assumption (Eq. 26) translates here as

$$\lim_{x \rightarrow \pm\infty} U_k(x_k + x) = \Omega(|x|). \quad (46)$$

The remaining argument goes through just as before. The modified environment side action (Eq. 30),

$$S_k[q_k(t), A(t)] \equiv \int_0^\beta dt \left\{ \frac{m_k}{2} \dot{q}_k(t)^2 + U_k(q_k(t) - c_k A(t)) \right\}, \quad (47)$$

gives the following expression for the influence functional, analogous to Eq. 36,

$$I_k[\tilde{a}] = \int_{-\infty}^{\infty} dx \int_x^x \mathcal{D}q_k(t) e^{-S_k[q_k(t), \tilde{a}]} \quad (48)$$

$$= \int_{-\infty}^{\infty} dx \int_{x-c_k \tilde{a}}^{x-c_k \tilde{a}} \mathcal{D}x_k(t) e^{-S_k[x_k(t), 0]} \quad (49)$$

$$= \int_{-\infty}^{\infty} dx \int_x^x \mathcal{D}x_k(t) e^{-S_k[x_k(t), 0]} \quad (50)$$

$$\equiv I_k, \quad \text{which is independent of } \tilde{a}. \quad (51)$$

Here, in Eq. 49, we defined $x_k(t) \equiv q_k(t) - c_k \tilde{a}$ and we have used the relation $S_k[q_k(t), \tilde{a}] = S_k[x_k(t), 0]$ (Eq. 47).

Hence, just like in the case of the CL model, we again have that $I[\tilde{a}] \equiv I$ is independent of \tilde{a} . This again leads to the familiar CL-USC result (Eq. 22). This means that CL-USC result is valid for a larger class of open system model, namely for GCL2 model, as defined here.

IV. USC-MFGS FOR ZWANZIG MODEL

We will now study the USC-MFGS for the so-called Zwanzig model^{50–53}, which has been previously studied in the context of Brownian motion and barrier crossing problems. Let the full SE Hamiltonian for the Zwanzig model be given as $\hat{H}_{SE} = \hat{H}_S + \hat{H}_I$, where \hat{H}_S is the free system Hamiltonian and \hat{H}_I is given as

$$\hat{H}_I = \sum_k^N \left[\frac{\hat{p}_k^2}{2m_k} + U_k^{\text{free}}(\hat{q}_k) + \frac{c_k}{2} U_k(\hat{q}_k - \hat{A}) \right]. \quad (52)$$

Here $U_k^{\text{free}}(q_k)$ is an arbitrary free potential of the k th environment particle and $U_k(x)$ is as defined in Section III A, but with just one extra condition that $U_k(x)$ now has a unique global minima point at $x = x_k$ and if there is any other local minima at a point $x = y_k$, then we have, for some non-infinitesimal positive number λ ,

$$U_k(y_k) - U_k(x_k) \geq \lambda > 0. \quad (53)$$

In other words, we now assume that not only does $U_k(x)$ have a unique global minimum, but also that if the potential has any other local minima, then there is a non-infinitesimal energy difference between the global minimum and the local minima. The significance of this assumption will become clear shortly.

Note that in Section III A, the interaction potential was of the form $U_k(\hat{q}_k - c_k \hat{A})$ while here, it is of the form $c_k U_k(\hat{q}_k - \hat{A})$. Hence, the Zwanzig model is microscopically motivated to have a spring like interaction between the system and the environment particles. In fact, if $U_k(x)$ is a harmonic potential, then c_k can be interpreted as the stiffness constant of the corresponding spring. Also note that here, we have deliberately not added a counter term in the interaction Hamiltonian because any renormalization of the system's free Hamiltonian will be assumed here to be of physical origin.

Now, the path integral expression for the MFGS will be given exactly as in CL model (Eq. 7 and Eq. 8), where the

action associated with $I_k[A(t)]$ will now be given as

$$S_k[q_k(t), A(t)] \equiv \int_0^\beta dt \left\{ \frac{m_k}{2} \dot{q}_k(t)^2 + U_k^{\text{free}}(q_k(t)) + \frac{c_k}{2} U_k(q_k(t) - A(t)) \right\}. \quad (54)$$

In the USC limit (Eq. 15), for paths that contribute significantly to the path integral, the condition

$$q_k(t) = A(t) + x_k \quad (55)$$

will get strictly imposed here. This is because as discussed in the context of the GCL2 model, $U_k(x_k) = 0$ is defined as the global minima of the potential $U_k(x)$ (Eq. 45) and we have further assumed that for Zwanzig model, this global minimum is unique and has a non-infinitesimal energy difference from any other local minima that might be there (Eq. 53). Hence, in the USC limit, we will have

$$\lim_{c_k \rightarrow \infty} \exp\{-c_k U_k(x)\} = \begin{cases} 0 & \text{for } x \neq x_k \\ 1 & \text{for } x = x_k \end{cases}. \quad (56)$$

Replacing Eq. 55 in Eq. 54, the corresponding influence functional (Eq. 8) becomes

$$I_k[A(t)] = e^{-\int_0^\beta dt \left\{ \frac{m_k}{2} \dot{A}(t)^2 + U_k^{\text{free}}(A(t) + x_k) \right\}}. \quad (57)$$

Since the influence functional $I_k[A(t)]$ (Eq. 8) arises when we take partial trace over the environment degrees of freedom, the environment side paths, $q_k(t)$, come with a constraint that $q_k(0) = q_k(\beta)$. In the USC limit, since $q_k(t)$ gets further constrained as $q_k(t) = A(t) + x_k$ (Eq. 55), this in turn puts a constraint that for paths that contribute to the path integral, $A(0) = A(\beta)$. This effectively diagonalizes the final USC-MFGS in the basis of system coupling operator \hat{A} , but through a mathematical mechanism that is different from the one encountered in the GCL model.

A. Special Case 1: Discrete system

If the system lives in a discrete Hilbert space, $A(t)$ generally has instantaneous jumps, in which case the kinetic term in the action in $I_k[A(t)]$ will blow up (Eq. 57), preventing the jump. Hence, for a discrete system, paths with an instantaneous jump will be suppressed and we will have $\dot{A}(t) = 0$.

Next, for $A(t) = \tilde{a}$, the influence functional (Eq. 57) simplifies as

$$\Rightarrow I_k[\tilde{a}] = \exp \left\{ -\int_0^\beta dt U_k^{\text{free}}(\tilde{a} + x_k) \right\} \quad (58)$$

$$= \exp \left\{ -\beta U_k^{\text{free}}(\tilde{a} + x_k) \right\}. \quad (59)$$

Replacing this in the full MFGS path integral expression (Eq. 7) gives

$$\hat{\rho}_{\text{USC}}(a, b) = \tilde{Z}^{-1} e^{-\beta U_{\text{eff}}(\tilde{a})} \int_a^b \mathcal{D}\phi(t) \exp \{-S_S[\tilde{a}, \phi(t)]\}. \quad (60)$$

Here a and b are the eigenvalues of the operator $\hat{\phi}$ and \tilde{a} is the eigenvalue⁵⁶ of \hat{A} and $U_{\text{eff}}(x)$ is defined as

$$U_{\text{eff}}(x) \equiv \sum_{k=1}^N U_k^{\text{free}}(x + x_k). \quad (61)$$

Finally, the USC-MFGS is given as,

$$\Rightarrow \hat{\rho}_{\text{USC}} = Z^{-1} \exp \{-\beta \tilde{H}\} \quad (62)$$

$$\tilde{H} \equiv \sum_i \hat{P}_i (\hat{H}_S + \hat{V}_0) \hat{P}_i. \quad (63)$$

Here \hat{P}_i is the projection operator on the i th degenerate subspaces of the operator \hat{A} with eigenvalue A_i . Here \hat{V}_0 is defined as

$$\hat{V}_0 = \sum_i U_{\text{eff}}(A_i) \hat{P}_i. \quad (64)$$

Hence, effectively, this is just the USC-MFGS result for GCL model, but with a renormalized free system Hamiltonian (Eq. 63).

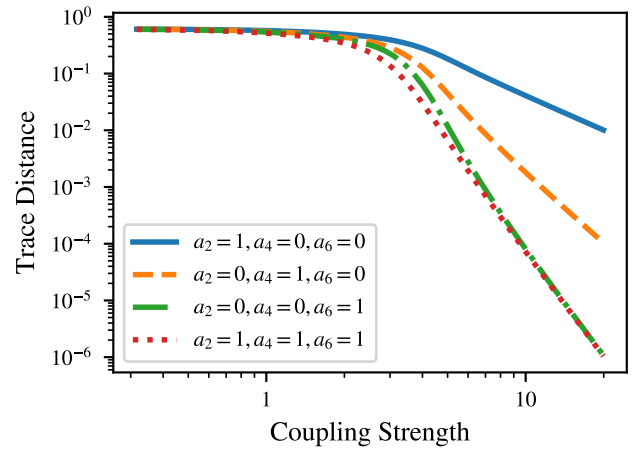


FIG. 2. The trace distance between the USC-MFGS for the GCL2 model and numerically evaluated MFGS as a function of the coupling strength c , for different choices of the interaction potential (Eq. 73).

B. Special Case 2: Continuous Variable system

Now, assume that we are dealing with a CV system, where we have a particle with mass m in a potential $V(q)$. Then, the free Hamiltonian \hat{H}_S is given as

$$\hat{H}_S = \frac{\hat{p}^2}{2m} + V(\hat{q}). \quad (65)$$

Also, for simplicity, assume that the system coupling-operator is given as $\hat{A} = \hat{q}$. Then, using the simplified expression for the influence functional for Zwanzig model (Eq. 57) in the full

MFGS path integral (Eq. 7) gives the USC-MFGS as

$$\hat{\rho}_{\text{USC}}(x, y) = \tilde{Z}^{-1} \delta(x, y) \int_x^y \mathcal{D}q(t) \exp \left\{ - \int_0^\beta dt \left(\frac{1}{2} M_{\text{eff}} \dot{q}(t)^2 + V_{\text{eff}}(q(t)) \right) \right\} \quad (66)$$

where,

$$M_{\text{eff}} = m + \sum_k m_k \quad (67)$$

$$V_{\text{eff}}(x) = V(x) + U_{\text{eff}}(x) \quad (68)$$

The USC-MFGS can now be determined as

$$\langle q | \rho_{\text{USC}} | q' \rangle = Z^{-1} \delta(q, q') \langle q | e^{-\beta \hat{H}_{\text{eff}}} | q' \rangle, \quad (69)$$

$$\hat{H}_{\text{eff}} = \frac{\hat{p}^2}{2M_{\text{eff}}} + V_{\text{eff}}(\hat{q}). \quad (70)$$

Note one key distinction here from the GCL2-USC result, in that although both the states are diagonal in the basis set by the system coupling-operator, the corresponding GCL2-USC result for CV system would be of the form, $\rho_{\text{USC-GCL2}} = Z^{-1} e^{-\beta V_{\text{eff}}(q)}$, as derived in Appendix. D.^{45,47,55} The Zwanzig-USC result (Eq. 69) will converge to the GCL2 result only when $M_{\text{eff}} \rightarrow \infty$, which will suppress paths of the type $\dot{q}(t) \neq 0$ in the path integral. This will typically not be the case for a system interacting with a few environment particles or particles that are not very massive, for example.

We note that there has been a disagreement in the literature regarding the form of the USC equilibrium state under the CL model.⁴⁵ For the CL model, Kawai et al. conjectured^{59,60} the system's dynamical state at long times to be $\rho^{\text{conj}} = \sum_i \hat{P}_i e^{-\beta \hat{H}_0} \hat{P}_i$ and we note that, coincidentally, the Zwanzig-USC result for CV systems (Eq. 69) is similar to this conjectured form.

V. NUMERICAL VERIFICATION

In this section, we conduct numerical tests to validate the analytical results presented in this paper. Specifically, we verify the USC-MFGS results for both the GCL2 (Eq. 22) and the Zwanzig model (Eq. 62). Additionally, we examine how the convergence rate of the MFGS towards the USC results varies with an increase in the SE coupling, across different model parameters.

For both the GCL2 and Zwanzig model, we consider a simplified scenario involving a qutrit system interacting with a single environmental particle. This allows for the convenient numerical evaluation of the exact MFGS, denoted by $\hat{\rho}_{\text{num}}$ (see Appendix. C for numerical details). By increasing the coupling strength, we can then compare the approach of $\hat{\rho}_{\text{num}}$ to the corresponding $\hat{\rho}_{\text{USC}}$ derived in this paper. We note that the system MFGS will get closer to the USC-result if multiple environment particles are simultaneously made to interact it.

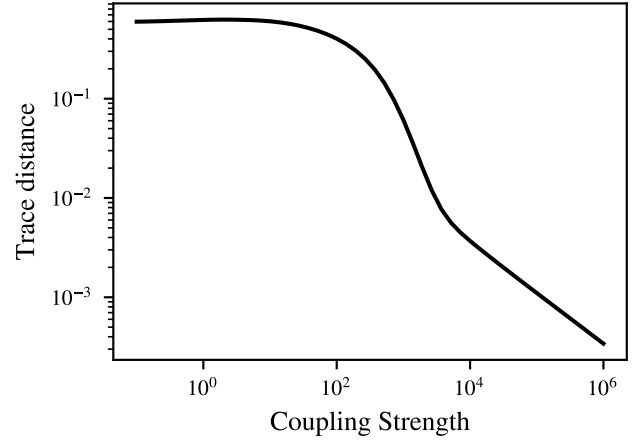


FIG. 3. The trace distance between the USC-MFGS for the Zwanzig model and the numerically calculated MFGS as a function of the coupling strength c .

The system free Hamiltonian, \hat{H}_S , and the system coupling-operator, \hat{A} , are fixed throughout to be

$$\hat{H}_S = \begin{pmatrix} 1 & 1 & 0 \\ 1 & 0 & 1 \\ 0 & 1 & -1 \end{pmatrix}, \quad \hat{A} = \begin{pmatrix} 1 & 0 & 0 \\ 0 & 0 & 0 \\ 0 & 0 & -0.5 \end{pmatrix}. \quad (71)$$

We set $\beta = 5E_h$ throughout, where we are working in the Hartree atomic units. For the GCL model, the interaction Hamiltonian, \hat{H}_I , (Eq. 24) simplifies as

$$\hat{H}_I = \frac{\hat{p}^2}{2M} + V(\hat{Q} - c\hat{A}). \quad (72)$$

Here $M = 1$ and $V(x)$ is assumed to be of the form

$$V(x) = \sum_{n=1}^3 a_{2n} x^{2n}. \quad (73)$$

Fig. 2 plots the trace distance between $\hat{\rho}_{\text{num}}$ and $\hat{\rho}_{\text{USC}}$ (Eq. 22) for this model as we increase the coupling parameter, c , for different values of the positive semi-definite coefficients a_{2n} . We generically find that, as expected, the trace distance drops quickly as the value of c is increased. We also find that higher order SE coupling causes the MFGS to approach the USC state faster as a function of the coupling parameter c .

This behavior can be explained for a generic GCL model if we note that a path $A(t)$ will contribute significantly to the path integral only if we have $\sigma_A = O(\Delta/c_k)$. For USC limit, we therefore require that $\Delta/c_k \ll 1$. Hence, the USC limit is approached based on the interplay between the coupling parameter c_k and Δ .⁶¹ So, if Δ is small for some coupling potential $V_k(x, y)$, like in the case of the potentials with $a_4 = 1$ or $a_6 = 1$ in Fig. 2, then it will facilitate the approach to the USC limit.

Next, for Zwanzig model, the interaction Hamiltonian \hat{H}_I (Eq. 52) is assumed to be

$$\hat{H}_I = \frac{\hat{p}^2}{2M} + U(\hat{Q}) + \frac{c}{2}(\hat{Q} - \hat{A})^2. \quad (74)$$

Here, again, $M = 1$ and $U(x)$ is a Morse potential

$$U(x) \equiv (1 - e^{-x})^2. \quad (75)$$

Fig. 3 plots the trace distance between $\hat{\rho}_{\text{num}}$ and $\hat{\rho}_{\text{USC}}$ (Eq. 62) for this model as we increase the value of the coupling parameter, c . We again observe that, as expected, the trace distance drops quickly as the value of c is increased, though the rate of approach to the USC result is much slower than the GCL case.

VI. CONCLUSION

The MFGS result, defined in Eq. 1, has been studied in USC limit for a system coupled to an anharmonic environment, hence going beyond the known USC result valid for the CL model. For all the generalized SE models studied, the USC-MFGS has been found to always be diagonal in the basis set by the SE interaction, although the exact form of the state differs from the CL-USC result, like in the case of a quite general class of models that we call the GCL model (Section III). We also identify a subclass of the GCL model, which we call the GCL2 model (Section III A), for which the USC-MFGS remains equivalent to the CL-USC result. Furthermore, for a so-called Zwanzig model (distinct from the GCL model) (Section IV), analytical expression for the USC state has been derived and is found to have qualitative differences from the GCL-USC result (Eq. 69).

These results demonstrate how the CL-USC result is influenced when the different assumptions of the model for which it was derived are relaxed one by one. In particular, these results directly extend the applicability of the CL-USC result for several strong coupling quantum thermodynamics, chemistry and biological problems where the anharmonicity of the environment becomes relevant. Also, our results indicate that anharmonicity of the environment has important implications on the rate of approach of the MFGS to the USC limit as a function of the coupling strength (Fig. 2). As a future direction, it would be interesting to apply our results to study some systems of physical interest (see for example^{34,41}).

The CL model has served as an important tool to model a variety of physical processes^{14–30}, and its strengths and limitations in capturing the properties of these systems of interest have also been investigated.^{42–44} Future research into extending such studies beyond the CL model (for example, to GCL2 and the Zwanzig model) will be of high interest. Moreover, the lines of reasoning used in this paper to obtain the USC-MFGS result can be applied to study USC-MFGS for other physically motivated generalized SE models.

Our results across a broad range of models indicate that the USC-MFGS invariably becomes diagonal in the basis of the system coupling-operator. Looking forward, it would be interesting to investigate whether this diagonalization is a universal feature of the USC-limit, independent of the further details of the SE model. Additionally, the CL-USC result has previously been expanded to first order in inverse of the SE coupling⁶² and has also been approximated for intermediate and weak

coupling regime.^{63,64} Extending these results beyond the CL model would be a valuable direction for future research.

AUTHOR DECLARATIONS

Conflict of Interest

The authors have no conflicts to disclose.

Author Contributions

Prem Kumar: Methodology (equal); Validation (equal); Formal analysis (equal); Investigation (equal); Conceptualization (equal); Writing – original draft (equal); Writing – review & editing (equal). **Sibasish Ghosh:** Methodology (equal); Validation (equal); Formal analysis (equal); Investigation (equal); Conceptualization (equal); Writing – original draft (equal); Writing – review & editing (equal).

DATA AVAILABILITY

The data that support the findings of this study are available within the article.

Appendix A: Proposition 1

Let $f(t)$ be a continuous, differentiable and square integrable function such that its derivative, $\dot{f}(t)$, is also square integrable, such that

$$f(t) \equiv g(t) + \varepsilon(t). \quad (A1)$$

Here $g(t)$ is also square integrable. Next, for some $\Delta > 0$, we have the constraint that

$$|\varepsilon(t)| < \Delta. \quad (A2)$$

Next, let us define

$$\langle g \rangle \equiv \frac{1}{\beta} \int_0^\beta dt g(t), \quad (A3)$$

$$\langle g^2 \rangle \equiv \frac{1}{\beta} \int_0^\beta dt g(t)^2, \quad (A4)$$

$$\sigma_g^2 \equiv \langle g^2 \rangle - \langle g \rangle^2. \quad (A5)$$

Then, in the limit $\sigma_g^2 \gg \Delta^2$, we will prove that

$$\frac{1}{\beta} \int_0^\beta dt \dot{f}(t)^2 \geq \mu \frac{\sigma_g^2}{\beta^2}, \quad (A6)$$

where $\mu > 0$ is a constant.

The intuitive idea behind the proof is as following. Part 1 of the proof consists of proving that

$$\lim_{\sigma_g^2 \gg \Delta^2} \sigma_f^2 \approx \sigma_g^2. \quad (\text{A7})$$

Part 2 then consists of proving that given σ_f ,

$$\frac{1}{\beta} \int_0^\beta dt \dot{f}(t)^2 \geq \mu \sigma_f^2 / \beta^2, \quad \text{where } \mu > 0. \quad (\text{A8})$$

Replacing Eq. A7 into Eq. A8 then gives the final result (Eq. A6).

Both these claims are intuitive, as the first claim states that if the absolute difference between two functions is much smaller than the standard deviation of one of the functions, then their standard deviations are also approximately equal. The second claim states that, for a function $f(t)$, if $\sigma_f^2 > 0$, then $\langle \dot{f}^2 \rangle > 0$ and also that $\langle \dot{f}^2 \rangle \propto \sigma_f^2$, which makes sense because if you scale a function as $f(t) \rightarrow 2f(t)$, then we have $\sigma_f^2 \rightarrow 4\sigma_f^2$ and $\langle \dot{f}^2 \rangle \rightarrow 4\langle \dot{f}^2 \rangle$.

Part 1 of the proof: Let us calculate σ_f^2 (using Eq. A1) as

$$\sigma_f^2 = \langle (g + \varepsilon)^2 \rangle - \langle g + \varepsilon \rangle^2 \quad (\text{A9})$$

$$= \langle g^2 \rangle + 2\langle g\varepsilon \rangle + \langle \varepsilon^2 \rangle - (\langle g \rangle^2 + 2\langle g \rangle \langle \varepsilon \rangle + \langle \varepsilon \rangle^2) \quad (\text{A10})$$

$$= \sigma_g^2 + \sigma_\varepsilon^2 + 2(\langle g\varepsilon \rangle - \langle g \rangle \langle \varepsilon \rangle) \quad (\text{A11})$$

$$\leq \sigma_g^2 + O(\Delta^2) + 2\sigma_g O(\Delta). \quad (\text{A12})$$

Here, we used $\langle g\varepsilon \rangle - \langle g \rangle \langle \varepsilon \rangle \leq \sigma_g \sigma_\varepsilon$ that can be derived using the Cauchy-Schwarz inequality. Finally, in the limit $\sigma_g^2 \gg \Delta^2$, we get the required result (Eq. A7).

Part 2 of the proof: Proof of Eq. A8 follows directly from Poincaré inequality^{65,66} that can be formally stated as following.⁶⁷

Poincaré inequality

Let Ω be an open, bounded, and connected subset of \mathbb{R}^d for some d and let $d\mathbf{x}$ denote d -dimensional Lebesgue measure on \mathbb{R}^d . Then the Poincaré inequality says that there exist constants C_1 and C_2 such that

$$\int_\Omega h^2(\mathbf{x}) d\mathbf{x} \leq C_1 \int_\Omega |\nabla h(\mathbf{x})|^2 d\mathbf{x} + C_2 \left[\int_\Omega h(\mathbf{x}) d\mathbf{x} \right]^2, \quad (\text{A13})$$

for all functions h in the Sobolev Space $H^1(\Omega)$ consisting of all functions in $L^2(\Omega)$ whose generalized derivatives are all also square integrable.

For 1-dimensional Euclidean space, for simplicity and without loss of any generality, let us redefine $f(t)$ such that

$\langle f \rangle = 0$. In other words, we shift $f(t) \rightarrow f(t) - \langle f \rangle$. Then, the Poincaré inequality implies that

$$\langle f^2 \rangle \leq C_1 \langle \dot{f}^2 \rangle + \beta C_2 \langle f \rangle^2 \quad (\text{A14})$$

$$\implies \sigma_f^2 \leq C_1 \langle \dot{f}^2 \rangle. \quad (\text{A15})$$

Since $\sigma_f^2 \geq 0$ and $\langle \dot{f}^2 \rangle \geq 0$, we have that C_1 is positive. We therefore have

$$\langle \dot{f}^2 \rangle \geq \frac{\beta^2 \sigma_g^2}{C_1 \beta^2}. \quad (\text{A16})$$

This proves Eq. A8 for $\mu = \beta^2/C_1$ and concludes the proof of the main result (Eq. A6) as well.

1. Proof of special case of Poincaré Inequality

Here, for completeness, we provide a proof for the special case of Poincaré inequality (Eq. A8), as per the present requirement. To simplify the proof, other than assuming that $\langle f \rangle = 0$, we also shift the range of the imaginary time from the conventional $0 \leq t \leq \beta$ to $-\beta/2 \leq t \leq \beta/2$. Now, given a constraint

$$\int_{-\beta/2}^{\beta/2} f(t)^2 dt = \beta \sigma_f^2, \quad (\text{A17})$$

we need to minimize over the action

$$S = \int_{-\beta/2}^{\beta/2} dt \dot{f}(t)^2. \quad (\text{A18})$$

We do this by perturbing the optimum path by a small amount, $f(t) \rightarrow f(t) + \delta(t)$, with $\delta(-\beta/2) = \delta(\beta/2) = 0$. Then Eq. A17 demands that to the first order in $\delta(t)$, we have

$$\int_{-\beta/2}^{\beta/2} f(t) \delta(t) dt = 0. \quad (\text{A19})$$

Now, the condition for the minimum action is $\delta S = 0$, where

$$\frac{\delta S}{2} = \int_{-\beta/2}^{\beta/2} dt \dot{f}(t) \dot{\delta}(t) \quad (\text{A20})$$

$$= \dot{f}(\beta/2) \delta(\beta/2) - \dot{f}(-\beta/2) \delta(-\beta/2) - \int_{-\beta/2}^{\beta/2} dt \ddot{f}(t) \delta(t) \quad (\text{A21})$$

$$= - \int_{-\beta/2}^{\beta/2} dt \ddot{f}(t) \delta(t) = 0. \quad (\text{A22})$$

Comparing Eq. A22 with Eq. A19, for some constant λ , we get

$$\ddot{f}(t) = \pm \lambda^2 f(t). \quad (\text{A23})$$

The solution of $f(t)$ can be of either sinusoidal or hyperbolic type. For the sinusoidal solution, we have

$$f(t) = A \sin(\lambda t + \phi). \quad (\text{A24})$$

Then the condition, $\langle f \rangle = 0$, demands that

$$\int_{-\frac{\beta}{2}}^{\frac{\beta}{2}} A \sin(\lambda t + \phi) dt = 0 \quad (\text{A25})$$

$$\Rightarrow -\frac{A}{\lambda} \left(\cos\left(\frac{\lambda\beta}{2} + \phi\right) - \cos\left(-\frac{\lambda\beta}{2} + \phi\right) \right) = 0 \quad (\text{A26})$$

$$\Rightarrow \cos\left(\frac{\lambda\beta}{2} + \phi\right) = \cos\left(-\frac{\lambda\beta}{2} + \phi\right). \quad (\text{A27})$$

The solution is either, for a generic λ , $\phi = 0$ or for a generic ϕ , $\lambda = 2\pi n/\beta$ for $n \in \mathbb{Z}$. Hence, we have

$$f(t) = \begin{cases} A \sin(\lambda t) & \text{for generic } \lambda \\ A \sin(\lambda t + \phi) & \text{for } \lambda = 2\pi n/\beta; \quad n \in \mathbb{Z} \end{cases}. \quad (\text{A28})$$

For hyperbolic solution, $f(t)$ is given as

$$f(t) = A \sinh(\lambda t). \quad (\text{A29})$$

Here, we do not have a cosh kind of term because of the requirement that $\langle f \rangle = \int_{-\beta/2}^{\beta/2} dt f(t) = 0$.

a. Sinusoidal solution

Let us first consider the solution for $\phi = 0$ and a generic λ

$$f(t) = A \sin(\lambda t) \quad (\text{A30})$$

$$\Rightarrow \beta \langle f^2 \rangle = A^2 \int_{-\frac{\beta}{2}}^{\frac{\beta}{2}} \sin^2(\lambda t) dt \quad (\text{A31})$$

$$= \frac{A^2}{2} \int_{-\frac{\beta}{2}}^{\frac{\beta}{2}} 1 - \cos(2\lambda t) dt \quad (\text{A32})$$

$$= \frac{A^2}{2} \left(\beta - \frac{2 \sin(\lambda\beta)}{2\lambda} \right) \quad (\text{A33})$$

$$= \frac{A^2\beta}{2} \left(1 - \frac{\sin(x)}{x} \right) \quad ; x \equiv \lambda\beta \quad (\text{A34})$$

$$\Rightarrow A^2 = \langle f^2 \rangle \frac{2x}{x - \sin(x)}. \quad (\text{A35})$$

This expression for A^2 is crucial, so let us also evaluate it for the case when, in Eq. A30, ϕ is present and $\lambda = 2\pi n/\beta$ for $n \in \mathbb{Z}$.

$$f(t) = A \sin\left(\frac{2\pi n t}{\beta} + \phi\right) \quad (\text{A36})$$

$$\Rightarrow \beta \langle f^2 \rangle = A^2 \int_{-\frac{\beta}{2}}^{\frac{\beta}{2}} \sin^2\left(\frac{2\pi n t}{\beta} + \phi\right) dt \quad (\text{A37})$$

$$= \frac{A^2\beta}{2} \quad (\text{A38})$$

$$\Rightarrow A^2 = 2 \langle f^2 \rangle \quad (\text{A39})$$

$$= \langle f^2 \rangle \frac{2x}{x - \sin(x)} \Big|_{x=2\pi n} \quad (\text{A40})$$

This is consistent with Eq. A35. Hence, Eq. A35 holds generically for the full sinusoidal case. Next, we have that

$$f(t)^2 + \frac{\dot{f}(t)^2}{\lambda^2} = A^2 \quad (\text{A41})$$

$$\Rightarrow \langle f^2 \rangle + \frac{\langle \dot{f}^2 \rangle}{\lambda^2} = A^2 \quad (\text{A42})$$

$$\Rightarrow \langle \dot{f}^2 \rangle = \lambda^2 (A^2 - \langle f^2 \rangle) \quad (\text{A43})$$

$$= \frac{x^2}{\beta^2} \left(\langle f^2 \rangle \frac{2x}{x - \sin(x)} - \langle f^2 \rangle \right) \quad (\text{A44})$$

$$= \frac{\langle f^2 \rangle}{\beta^2} x^2 \left(\frac{x + \sin(x)}{x - \sin(x)} \right) \quad (\text{A45})$$

$$\geq \left(\min_x h_{\sin}(x) \right) \frac{\langle f^2 \rangle}{\beta^2}. \quad (\text{A46})$$

Here

$$h_{\sin}(x) \equiv x^2 \left(\frac{x + \sin(x)}{x - \sin(x)} \right). \quad (\text{A47})$$

Note that $\min_x h_{\sin}(x) > 0$, which can also be seen from Fig. 4. Eq. A46 is the desired result for the sinusoidal case.

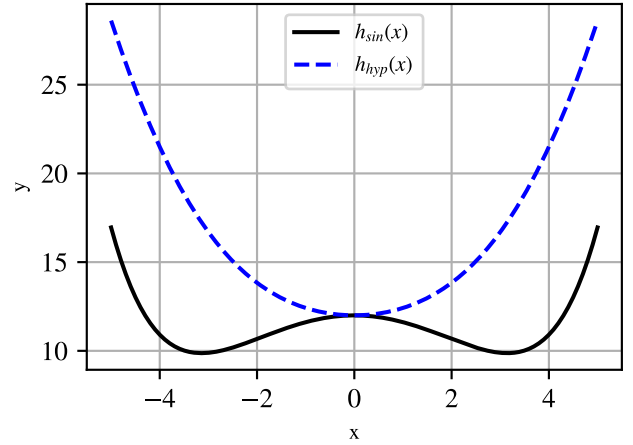


FIG. 4. Plot of $h_{\sin}(x)$ (Eq. A47) and $h_{\text{hyp}}(x)$ (Eq. A57), which demonstrates that the minima of both these functions are larger than zero.

b. Hyperbolic solution

Let

$$f(t) \equiv A \sinh(\lambda t) \quad (\text{A48})$$

$$\beta \langle f^2 \rangle \equiv A^2 \int_{-\frac{\beta}{2}}^{\frac{\beta}{2}} \sinh^2(\lambda t) dt \quad (\text{A49})$$

$$= -\frac{A^2}{2} \int_{-\frac{\beta}{2}}^{\frac{\beta}{2}} 1 - \cosh(2\lambda t) dt \quad (\text{A50})$$

$$\Rightarrow A^2 = -\langle f^2 \rangle \frac{2x}{x - \sinh(x)}. \quad (\text{A51})$$

Here, in the last step, we used the analogous derivation from Eq. A32 to Eq. A35, but with an extra minus sign. Now, note that we have

$$\frac{\dot{f}(t)^2}{\lambda^2} - f(t)^2 = A^2 \quad (\text{A52})$$

$$\implies \frac{\langle \dot{f}^2 \rangle}{\lambda^2} - \langle f^2 \rangle = A^2 \quad (\text{A53})$$

$$\implies \langle \dot{f}^2 \rangle = -\lambda^2 (-A^2 - \langle f^2 \rangle) \quad (\text{A54})$$

$$= -\frac{x^2}{\beta^2} \left(\langle f^2 \rangle \frac{2x}{x - \sinh(x)} - \langle f^2 \rangle \right) \quad (\text{A55})$$

$$\geq \left(\min_x h_{\text{hyp}}(x) \right) \frac{\langle f^2 \rangle}{\beta^2}. \quad (\text{A56})$$

In the last step, we used the analogous calculation from Eq. A44 to Eq. A46, with just an extra minus sign. Here, $h_{\text{hyp}}(x)$ is defined as

$$h_{\text{hyp}}(x) \equiv x^2 \left(\frac{\sinh(x) + x}{\sinh(x) - x} \right). \quad (\text{A57})$$

Note that $\min_x h_{\text{hyp}}(x) > 0$, which can also be seen from Fig. 4. Eq. A56 is the desired result for the hyperbolic case.

Appendix B: Proposition 2

Let $f(x)$ be a continuous, differentiable and square integrable function and let us define $h(x) \equiv \frac{d}{dx}f(x)$ such that

$$h(x) = \Omega(1). \quad (\text{B1})$$

Now, let $g(t)$ be another square integrable function and

$$\langle f \circ g \rangle \equiv \frac{1}{\beta} \int_0^\beta dt f(g(t)) \quad (\text{B2})$$

$$\langle (f \circ g)^2 \rangle \equiv \frac{1}{\beta} \int_0^\beta dt f(g(t))^2 \quad (\text{B3})$$

$$\sigma_{f \circ g}^2 \equiv \langle (f \circ g)^2 \rangle - \langle f \circ g \rangle^2. \quad (\text{B4})$$

Then, we will prove that

$$\sigma_{f \circ g}^2 \gtrsim \sigma_g^2, \quad (\text{B5})$$

where σ_g^2 is defined analogously (Eq. A5).

Proof: We first write

$$f(x_1) = f(x_0) + \int_{x_0}^{x_1} h(x') dx'. \quad (\text{B6})$$

Now, from Eq. B1, if $x_1 > x_0$, then

$$\int_{x_0}^{x_1} h(x') dx' \gtrsim x_1 - x_0 > 0 \quad (\text{B7})$$

$$\implies \int_{x_1}^{x_0} h(x') dx' \lesssim x_0 - x_1 < 0 \quad (\text{B8})$$

$$\implies \left| \int_a^b h(x') dx' \right| \gtrsim |b - a| \quad \forall a, b \quad (\text{B9})$$

$$\implies |f(b) - f(a)| \gtrsim |b - a|. \quad (\text{B10})$$

Then we have

$$|(f \circ g)(t_1) - (f \circ g)(t_2)| \gtrsim |g(t_1) - g(t_2)| \quad \forall t_1, t_2. \quad (\text{B11})$$

Now, let t' be the time at which we have $(f \circ g)(t') = \langle f \circ g \rangle$. Then we have

$$\sigma_{f \circ g}^2 = \frac{1}{\beta} \int_0^\beta dt ((f \circ g)(t) - (f \circ g)(t'))^2 \quad (\text{B12})$$

$$\gtrsim \frac{1}{\beta} \int_0^\beta dt (g(t) - g(t'))^2 \quad (\text{B13})$$

$$= \frac{1}{\beta} \int_0^\beta dt (g(t) - (\langle g \rangle + c))^2 \text{ where } c \equiv g(t') - \langle g \rangle \quad (\text{B14})$$

$$= \frac{1}{\beta} \int_0^\beta dt [(g(t) - \langle g \rangle)^2 + c^2 - 2c(g(t) - \langle g \rangle)] \quad (\text{B15})$$

$$= \sigma_g^2 + c^2 - 2c(\langle g \rangle - \langle g \rangle) \quad (\text{B16})$$

$$\geq \sigma_g^2 \quad (\text{B17})$$

$$\implies \sigma_{f \circ g}^2 \gtrsim \sigma_g^2. \quad (\text{B18})$$

Appendix C: Numerical evaluation of the MFGS for qutrit system coupled to single anharmonic oscillator at finite SE coupling

The Hamiltonian of a qutrit system coupled to a single anharmonic oscillator (Eq. 71 together with Eq. 72 (for GCL2 model) and Eq. 74 (for Zwanzig-model)) is essentially an infinite-dimensional operator. In order to numerically evaluate the MFGS,

$$\hat{\rho} = Z^{-1} \text{Tr}_E \left[e^{-\beta \hat{H}_{\text{SE}}} \right], \quad (\text{C1})$$

we truncate the position operator \hat{Q} of environment oscillator so that its eigenvalues Q is restricted to $Q_{\min} \leq Q \leq Q_{\max}$. We also discretize \hat{Q} into N discrete points. This effectively approximates the original infinite-dimensional Hamiltonian \hat{H}_{SE} to one with $3N$ dimensions.

It is now possible to numerically evaluate the MFGS (Eq. C1). We vary the values of Q_{\min}, Q_{\max} and N until the final result of interest converges (in this case, the trace distance between $\hat{\rho}_{\text{num}}$ and $\hat{\rho}_{\text{USC}}$).

Appendix D: USC-MFGS for CV system for CL model

In the case of a CV system, if we consider the free Hamiltonian \hat{H}_S to be given by

$$\hat{H}_S = \frac{\hat{p}^2}{2m} + V(\hat{q}), \quad (D1)$$

with $\hat{A} \equiv \hat{q}$, then the projectors \hat{P}_i in Eq. 23 will be replaced by $|q\rangle\langle q|$ and the summation over i will be replaced by an integral over the eigenvalue q , giving rise to

$$\tilde{H} = \int dq \langle q | \hat{H}_S | q \rangle |q\rangle\langle q| \quad (D2)$$

$$= \int \frac{1}{2m} \langle q | \hat{p}^2 | q \rangle |q\rangle\langle q| dq + \int V(q) |q\rangle\langle q| dq. \quad (D3)$$

Since both the terms in Eq. D3 commute with each other, the corresponding USC-MFGS (Eq. 22) is given as

$$\hat{\rho}_{\text{USC}} = Z^{-1} \exp \{ -\beta \tilde{H} \} \quad (D4)$$

$$= Z^{-1} e^{-\beta V(\hat{q})} \exp \left\{ -\frac{\beta}{2m} \int \langle q | \hat{p}^2 | q \rangle |q\rangle\langle q| dq \right\}. \quad (D5)$$

Now, we have $\langle q | \hat{p}^2 | q \rangle = \langle q + a | \hat{p}^2 | q + a \rangle$, for all real a . Therefore, $\exp \left\{ -\frac{\beta}{2m} \int \langle q | \hat{p}^2 | q \rangle |q\rangle\langle q| dq \right\}$ is proportional to the identity operator, and hence can be absorbed into the trace. We therefore get the USC-MFGS for CV system as⁴⁷

$$\hat{\rho}_{\text{USC}} = Z'^{-1} e^{-\beta V(\hat{q})}. \quad (D6)$$

REFERENCES

- ¹H. J. D. Miller, “Hamiltonian of mean force for strongly-coupled systems,” in *Thermodynamics in the Quantum Regime: Fundamental Aspects and New Directions*, edited by F. Binder, L. A. Correa, C. Gogolin, J. Anders, and G. Adesso (Springer International Publishing, Cham, 2018) pp. 531–549.
- ²J. G. Kirkwood, “Statistical mechanics of fluid mixtures,” *The Journal of Chemical Physics* **3**, 300–313 (1935).
- ³T. W. Allen, O. S. Andersen, and B. Roux, “Molecular dynamics—potential of mean force calculations as a tool for understanding ion permeation and selectivity in narrow channels,” *Biophysical Chemistry* **124**, 251–267 (2006).
- ⁴K. Maksimiak, S. Rodziewicz-Motowidło, C. Czaplewski, A. Liwo, and H. A. Scheraga, “Molecular simulation study of the potentials of mean force for the interactions between models of like-charged and between charged and nonpolar amino acid side chains in water,” *The Journal of Physical Chemistry B* **107**, 13496–13504 (2003).
- ⁵B. Roux and T. Simonson, “Implicit solvent models,” *Biophysical Chemistry* **78**, 1–20 (1999).
- ⁶B. Roux, “The calculation of the potential of mean force using computer simulations,” *Computer Physics Communications* **91**, 275–282 (1995).
- ⁷U. Seifert, “First and second law of thermodynamics at strong coupling,” *Physical Review Letters* **116**, 020601 (2016).
- ⁸T. G. Philbin and J. Anders, “Thermal energies of classical and quantum damped oscillators coupled to reservoirs,” *Journal of Physics A: Mathematical and Theoretical* **49**, 215303 (2016).
- ⁹C. Jarzynski, “Nonequilibrium work theorem for a system strongly coupled to a thermal environment,” *Journal of Statistical Mechanics: Theory and Experiment* **2004**, P09005 (2004).
- ¹⁰M. Campisi, P. Talkner, and P. Hänggi, “Fluctuation theorem for arbitrary open quantum systems,” *Physical Review Letters* **102**, 210401 (2009).
- ¹¹Á. Rivas, “Strong coupling thermodynamics of open quantum systems,” *Physical Review Letters* **124**, 160601 (2020).
- ¹²P. Talkner and P. Hänggi, “Colloquium: Statistical mechanics and thermodynamics at strong coupling: Quantum and classical,” *Reviews of Modern Physics* **92**, 041002 (2020).
- ¹³P. Strasberg and M. Esposito, “Measurability of nonequilibrium thermodynamics in terms of the Hamiltonian of mean force,” *Physical Review E* **101**, 050101 (2020).
- ¹⁴R. P. Feynman and F. Vernon Jr, “The theory of a general quantum system interacting with a linear dissipative system,” *Annals of Physics* **281**, 547–607 (2000).
- ¹⁵A. J. Leggett, S. Chakravarty, A. T. Dorsey, M. P. Fisher, A. Garg, and W. Zwerger, “Dynamics of the dissipative two-state system,” *Reviews of Modern Physics* **59**, 1 (1987).
- ¹⁶J. B. Gilmore and R. H. McKenzie, “Criteria for quantum coherent transfer of excitations between chromophores in a polar solvent,” *Chemical Physics Letters* **421**, 266–271 (2006).
- ¹⁷A. Nazir, “Correlation-dependent coherent to incoherent transitions in resonant energy transfer dynamics,” *Physical Review Letters* **103**, 146404 (2009).
- ¹⁸D. Xu and K. Schulten, “Coupling of protein motion to electron transfer in a photosynthetic reaction center: investigating the low temperature behavior in the framework of the spin–boson model,” *Chemical Physics* **182**, 91–117 (1994).
- ¹⁹A. Ishizaki and G. R. Fleming, “Unified treatment of quantum coherent and incoherent hopping dynamics in electronic energy transfer: Reduced hierarchy equation approach,” *The Journal of Chemical Physics* **130** (2009), 10.1063/1.3155372.
- ²⁰P. Rebentrost, M. Mohseni, I. Kassal, S. Lloyd, and A. Aspuru-Guzik, “Environment-assisted quantum transport,” *New Journal of Physics* **11**, 033003 (2009).
- ²¹I. de Vega, “Non-markovian stochastic schrödinger description of transport in quantum networks,” *Journal of Physics B: Atomic, Molecular and Optical Physics* **44**, 245501 (2011).
- ²²M. Mohseni, A. Shabani, S. Lloyd, Y. Omar, and H. Rabitz, “Geometrical effects on energy transfer in disordered open quantum systems,” *The Journal of Chemical Physics* **138** (2013), 10.1063/1.4807084.
- ²³J. Tang, “Effects of a fluctuating electronic coupling matrix element on electron transfer rate,” *The Journal of Chemical*

- Physics **98** (1993), 10.1063/1.464820.
- ²⁴P. F. Barbara, T. J. Meyer, and M. A. Ratner, “Contemporary issues in electron transfer research,” *The Journal of Physical Chemistry* **100** (1996), 10.1021/jp9605663.
 - ²⁵M. G. Mavros, D. Hait, and T. Van Voorhis, “Condensed phase electron transfer beyond the condon approximation,” *The Journal of Chemical Physics* **145** (2016), 10.1063/1.4971166.
 - ²⁶X. Zhao, W. Shi, L.-A. Wu, and T. Yu, “Fermionic stochastic Schrodinger equation and master equation: An open-system model,” *Physical Review A* **86** (2012), 10.1103/physreva.86.032116.
 - ²⁷Y. Tanimura and S. Mukamel, “Two-dimensional femtosecond vibrational spectroscopy of liquids,” *The Journal of Chemical Physics* **99** (1993), 10.1063/1.465484.
 - ²⁸U. Weiss, *Quantum dissipative systems* (World Scientific, 2012).
 - ²⁹H. P. Breuer and F. Petruccione, *The theory of open quantum systems* (Oxford University Press, Great Clarendon Street, 2002).
 - ³⁰C. Gardiner and P. Zoller, *Quantum noise: a handbook of Markovian and non-Markovian quantum stochastic methods with applications to quantum optics* (Springer Science & Business Media, 2004).
 - ³¹A. Bose and P. L. Walters, “Impact of spatial inhomogeneity on excitation energy transport in the fenna–matthews–olson complex,” *The Journal of Physical Chemistry B* **127**, 7663–7673 (2023).
 - ³²K. Okumura and Y. Tanimura, “Unified time-path approach to the effect of anharmonicity on the molecular vibrational spectroscopy in solution,” *The Journal of Chemical Physics* **105**, 7294–7309 (1996).
 - ³³D. G. Evans, “Anharmonic effects in photoinduced electron transfer,” *The Journal of Chemical Physics* **113**, 3282–3288 (2000).
 - ³⁴H. Wang and M. Thoss, “Semiclassical simulation of absorption spectra for a chromophore coupled to an anharmonic bath,” *Chemical Physics* **304**, 121–131 (2004).
 - ³⁵D. M. Lockwood, M. A. Ratner, and R. Kosloff, “Effects of anharmonicity and electronic coupling on photoinduced electron transfer in mixed valence compounds,” *The Journal of Chemical Physics* **117**, 10125–10132 (2002).
 - ³⁶F. Wang and N. Makri, “Quantum-classical path integral with a harmonic treatment of the back-reaction,” *The Journal of Chemical Physics* **150** (2019), 10.1063/1.5091725.
 - ³⁷G. Ilk and N. Makri, “Real time path integral methods for a system coupled to an anharmonic bath,” *The Journal of Chemical Physics* **101** (1994), 10.1063/1.468364.
 - ³⁸Q. Shi and E. Geva, “A semiclassical generalized quantum master equation for an arbitrary system-bath coupling,” *The Journal of Chemical Physics* **120** (2004), 10.1063/1.1738109.
 - ³⁹I. Ohmine and H. Tanaka, “Fluctuation, relaxations, and hydration in liquid water. hydrogen-bond rearrangement dynamics,” *Chemical reviews* **93**, 2545–2566 (1993).
 - ⁴⁰M. Thoss and H. Wang, “Quantum dynamical simulation of ultrafast molecular processes in the condensed phase,” *Chemical Physics* **322**, 210–222 (2006).
 - ⁴¹H. Wang and M. Thoss, “Quantum dynamical simulation of electron-transfer reactions in an anharmonic environment,” *The Journal of Physical Chemistry A* **111**, 10369–10375 (2007).
 - ⁴²M. Bramberger and I. De Vega, “Dephasing dynamics of an impurity coupled to an anharmonic environment,” *Physical Review A* **101**, 012101 (2020).
 - ⁴³A. Rognoni, R. Conte, and M. Ceotto, “Caldeira-Leggett model vs ab initio potential: A vibrational spectroscopy test of water solvation,” *The Journal of Chemical Physics* **154** (2021).
 - ⁴⁴F. Gottwald, S. D. Ivanov, and O. Kuhn, “Applicability of the Caldeira-Leggett model to vibrational spectroscopy in solution,” *The Journal of Physical Chemistry Letters* **6**, 2722–2727 (2015).
 - ⁴⁵J. Cresser and J. Anders, “Weak and ultrastrong coupling limits of the quantum mean force gibbs state,” *Physical Review Letters* **127**, 250601 (2021).
 - ⁴⁶A. Trushechkin, M. Merkli, J. Cresser, and J. Anders, “Open quantum system dynamics and the mean force gibbs state,” *AVS Quantum Science* **4** (2022).
 - ⁴⁷J. Ankerhold, “Phase space dynamics of overdamped quantum systems,” *Europhysics Letters* **61**, 301 (2003).
 - ⁴⁸S. Hilt, B. Thomas, and E. Lutz, “Hamiltonian of mean force for damped quantum systems,” *Physical Review E* **84**, 031110 (2011).
 - ⁴⁹A. Trushechkin, “Quantum master equations and steady states for the ultrastrong-coupling limit and the strong-decoherence limit,” *Physical Review A* **106**, 042209 (2022).
 - ⁵⁰R. Zwanzig, “Nonlinear generalized Langevin equations,” *Journal of Statistical Physics* **9**, 215–220 (1973).
 - ⁵¹D. Banerjee, B. C. Bag, S. K. Banik, and D. S. Ray, “Approach to quantum Kramers’ equation and barrier crossing dynamics,” *Physical Review E* **65** (2002), 10.1103/physreve.65.021109.
 - ⁵²D. Banerjee, S. K. Banik, B. C. Bag, and D. S. Ray, “Quantum Kramers’ equation for energy diffusion and barrier crossing dynamics in the low-friction regime,” *Physical Review E* **66** (2002), 10.1103/physreve.66.051105.
 - ⁵³D. Barik, S. K. Banik, and D. S. Ray, “Quantum phase-space function formulation of reactive flux theory,” *The Journal of Chemical Physics* **119**, 680–695 (2003).
 - ⁵⁴R. Feynman and A. Hibbs, *The path integral formulation of quantum mechanics*, McGraw-Hill, New York (1965).
 - ⁵⁵P. Kumar, “Local harmonic approximation to quantum mean force gibbs state,” arXiv preprint arXiv:2401.11595 (2024).
 - ⁵⁶Since \hat{A} and $\hat{\phi}$ commute, let, in the above equation, $|a, a'\rangle$ and $|b, b'\rangle$ be the corresponding eigenvectors of $\hat{\phi}$ and \hat{A} with eigenvalues a, b and a', b' , respectively. Then, if $a' \neq \tilde{a}$ or $b' \neq \tilde{a}$, then, as remarked in Sec. II, for the corresponding action we have, $S_S[\tilde{a}, \phi(t)] = \infty$, effectively making $\hat{\rho}_{\text{USC}}$ diagonal in the basis of \hat{A} .
 - ⁵⁷C. Bhadra and D. Banerjee, “System-reservoir theory with anharmonic baths: a perturbative approach,” *Journal of Statistical Mechanics: Theory and Experiment* **2016**, 043404 (2016).
 - ⁵⁸D. E. Knuth, “Big omicron and big omega and big theta,” *ACM Sigact News* **8**, 18–24 (1976).

- ⁵⁹K. Goyal and R. Kawai, “Steady state thermodynamics of two qubits strongly coupled to bosonic environments,” *Physical Review Research* **1**, 033018 (2019).
- ⁶⁰P. L. Orman and R. Kawai, “A qubit strongly interacting with a bosonic environment: Geometry of thermal states,” arXiv preprint arXiv:2010.09201 (2020).
- ⁶¹ Δ quantifies, for the potential $V_k(x, y)$, for a fixed value of y , a (possibly) arbitrarily large but finite length scale about the global minima point $x = \tilde{x}(y)$ such that for $|x - \tilde{x}(y)| > \Delta$, the value of the potential $V_k(x, y)$ is so large that it does not influence the MFGS path integral.
- ⁶²C. Latune, “Steady state in ultrastrong coupling regime: Expansion and first orders,” *Quanta* **11**, 53–71 (2022).
- ⁶³N. Anto-Sztrikacs, A. Nazir, and D. Segal, “Effective-hamiltonian theory of open quantum systems at strong coupling,” *PRX Quantum* **4**, 020307 (2023).
- ⁶⁴N. Anto-Sztrikacs, B. Min, M. Brenes, and D. Segal, “Effective hamiltonian theory: An approximation to the equilibrium state of open quantum systems,” *Physical Review B* **108**, 115437 (2023).
- ⁶⁵G. Leoni, *A first course in Sobolev spaces*, Vol. 181 (American Mathematical Society, 2024).
- ⁶⁶L. C. Evans, *Partial differential equations*, Vol. 19 (American Mathematical Society, 2022).
- ⁶⁷C. Stover, “Poincaré inequality,” MathWorld-A Wolfram Web Resource, created by Eric W. Weisstein.